Journal of Fluorescence (2020) 30:463–470
https://doi.org/10.1007/s10895-020-02512-3

ORIGINAL ARTICLE

Calcium Ions Turn on the Fluorescence of Oxytetracycline for Sensitive and Selective Detection

Hongxia Chen[1] · Junxiang Peng[1] · Long Yu[1] · Hui Chen[1] · Mingtai Sun[3,4] · Zhenli Sun[1] · Runyan Ni[2,3,4] · Khalid A. Alamry[5] · Hadi M. Marwani[5] · Suhua Wang[1,2,3,5]

Received: 18 November 2019 / Accepted: 14 February 2020 / Published online: 6 March 2020

Abstract

Herein, we report an interesting finding about the new application of oxytetracycline (OTC), as a fluorescent probe for the detection of calcium ion (Ca^{2+}), which proved that it can offer an expeditious, highly sensitive, and selective detection method for Ca^{2+}. Upon the addition of Ca^{2+}, the fluorescence of OTC could be significantly enhanced with rapid response and high sensitivity, and achieved a good limit of detection as low as 125 nM in aqueous solution. The complex formed via Ca^{2+} coordinating to the hydroxyl group of OTC contributes to the fluorescence enhancement, which has been proved by several characterization methods including UV-vis analysis, binding constant determination, and fluorescence titration. The method avoided complexity for EDTA measurement of Ca^{2+} in running water as proposed previously. Taking advantage of good availability, stability and operability, the OTC was further successfully applied to the detection of Ca^{2+} in a real environment.

Keywords Oxytetracycline (OTC) · Fluorescent probe · Calcium ions · Calcium complex · Coordination

Introduction

Calcium ions (Ca^{2+}) are widely found in disparate fields, such as industry and agriculture, [1] and have been recognized as a highly important element for life [2, 3]. Advanced detection techniques for Ca^{2+} such as capillary electrophoresis, [4] inductively coupled plasma atomic emission spectrometry [5] and mass spectrometry [6] have been developed. In addition, the method of titration has been widely used for Ca^{2+} determination in the past decades [7–10]. At first, Ca^{2+} separated from the magnesium was determined by ethylene diamine tetraacetic acid (EDTA) titration. Then, the influence of masking agents and indicators on the chelatometric determination of Ca^{2+} was investigated [11]. This well-known technology, however, is often limited by the low selectivity and complexity of the detection process based on the intrinsic complexation response [12, 13]. Traditionally, the endpoint was indicated with ion-selective electrodes by Eriochrome Black T for calcium titration at pH 10 [14–16]. Griko studied the correlation titration reaction between Ca^{2+} and EDTA, and obtained the strong dependence of binding thermodynamics on reaction in the buffer [17]. Therefore, it is of great importance to develop a unique and facile system for the detection of low-concentration of Ca^{2+}.

Oxytetracycline (OTC), a compound belongs to the tetracycline family, is known to be a basic medicinal antibiotic substance in life [18–20]. As a broad-spectrum antibiotic, it has been used in clinical application for the treatment or prevention of infections in bovine, pig, poultry, and fish

✉ Mingtai Sun
mtsun@gdupt.edu.cn

✉ Runyan Ni
runyan.ni@nusri.cn

✉ Suhua Wang
wangsuhua@ncepu.edu.cn

1 MOE Key Laboratory of Resources and Environmental System Optimization, College of Environmental Science and Engineering, North China Electric Power University, Beijing 102206, People's Republic of China

2 College of Environmental Science and Engineering, North China Electric Power University, Beijing 102206, China

3 Guangdong Provincial Key Laboratory of Petrochemcial Pollution Processes and Control, School of Environmental Science and Engineering, Guangdong University of Petrochemical Technology, Maoming 525000, People's Republic of China

4 National University of Singapore (Suzhou) Research Institute, 377 Linquan Street, Suzhou, Jiangsu 215123, People's Republic of China

5 Department of Chemistry, Faculty of Science, King Abdulaziz University, Jeddah 21589, Saudi Arabia

productions [21–23]. And it also has been widely used in agriculture and animal husbandry as a growth promoter or bacterial infection inhibitor against a wide range of Gram-positive and Gram-negative bacteria based on the inhibition of bacterial protein synthesis [24, 25]. OTC is an amphoteric compound with unique structure of the presence of both Lewis base and Lewis acid functional groups. The location of donor group allows tetracycline being an applicable ligand to chelate with metal ions [26].

Taking advantage of the specific performance of OTC, we developed a new convenient and sensitive system for the detection of Ca^{2+} using a turn on probe. The probe OTC has extremely weak measurable fluorescence in the organic solvent of N,N-dimethylformamide (DMF), a polar inert solvent, which is a very versatile solvent with wide industrial applications [27]. While maintaining a stable molecular state, the reaction product of OTC and Ca^{2+} also has good solubility and chemical stability. And the addition of Ca^{2+} leads to the OTC to produce an enhanced fluorescence response, which shows a stable and rapid response in a narrow range of calcium concentration.

Experimental Section

Materials and Reagents

Oxytetracycline (OTC) dihydrate ($C_{22}H_{24}N_2O_9{\cdot}2H_2O$), N,N-Dimethylformamide (DMF), dimethyl sulfoxide (DMSO), acetonitrile, dichloromethane, acetone, isopropanol, L-ascorbic acid (Vc), L-histidine (His) were purchased from Aladdin Chemistry Co. Ltd. (Shanghai, China). Absolute ethanol and methanol were got from Beijing Chemical Works. Calcium chloride ($CaCl_2$), sodium chloride (NaCl), potassium chloride (KCl), barium chloride ($BaCl_2$), sodium nitrate ($NaNO_3$), sodium bicarbonate ($NaHCO_3$), sodium sulfate (Na_2SO_4) and iron chloride ($FeCl_3$), mercuric chloride ($HgCl_2$), manganese chloride ($MnCl_2$), lead nitrate ($Pb(NO_3)_2$), nickel chloride ($NiCl_2$), cupric chloride ($CuCl_2$) and ammonium chloride (NH_4Cl) were purchased from Sinopharm Chemical Reagent Co. Ltd. All reagents and solvents selected were used directly without further purification. Ultrapure water (18.2 MΩ·cm) was taken from the Millipore water purification system. The fluorescent cuvette was washed twice with ethanol and then dried before use.

Apparatus and Methods

Fluorescence measurements were carried out on a F-7100 Fluorescence spectrometer (HITACHI, Japan) with excitation and emission slit widths of 10 mm. UV-vis absorption was determined at a Shimadzu UV-2550 spectrometer at room temperature. Fourier transformed infrared (FTIR) spectra of OTC and $CaCl_2$ were performed on the FTIR spectrophotometer. The model of the electronic balance used in the experiment was FA2204N (Shanghai Jinghai Instrument Co.Ltd.). Freeze dryer (FD-1A-50, Beijing BIOCOOL Experimental Instrument Co.Ltd) was prepared for the preparation of composite solid samples.

Fluorescence Responses to Ca^{2+}

When DMF solution was used as the detection environment, the strong polarity of the DMF not only makes the OTC have good solubility, but also makes the response of OTC and Ca^{2+} more stable. The experimental error was reduced by formulating the OTC probe into a 1 mM stock solution in methanol, [28] while weighing the anhydrous calcium chloride to obtain a 1 mM stock solution in water for use, and then diluting the different stock solutions for later use. Typically, 6 μL of the OTC solution was injected into 1994 μL of DMF in a quartz fluorescence cuvette to give a final concentration of 3 μM. The response was recorded after Ca^{2+} was added to the probe solution under the same conditions. The final concentrations of Ca^{2+} were 0, 0.5, 1, 1.5, 2, 2.5, 3, 4, and 5 μM, respectively. All fluorescence spectra were chosen to be excited at 365 nm. The scan rate is the default value of 1200 nm min^{-1}.

Fluorescence Responses to Biological Reagents and Metal Ions

As is known to us, heavy metal ions or other biological reagents are abundant in domestic tap water environments with a small concentration, while the hydroxyl functional groups on OTC and the position of hydrogen ions can rapidly coordinate with many metal ions, so it is necessary to study the selectivity and anti-interference ability of OTC to other metal ions. Among them, Na^+, K^+, Ca^{2+}, Ba^{2+} and Fe^{3+} were selected as typical ions. The effect of other not typical ions such as Hg^{2+}, Mn^{2+}, Pb^{2+}, Ni^{2+}, Cu^{2+} and NH_4^+ were also evaluated. In addition, it includes anionic carbonate (CO_3^{2-}), bicarbonate (HCO_3^-), sulfate (SO_4^{2-}), nitrate (NO_3^-) and chloride (Cl^-), which are often present in water. In addition, several amino acids were investigated as representative interferences, such as L-ascorbic acid (Vc) and L-histidine (His).

Results and Discussion

Optimal Conditions of Solution Environment

The performance of OTC in the following solution environments, including ultrapure water, Tris buffer (10 mM), ethanol solution, DMF, DMSO, acetonitrile, dichloromethane, acetone, and isopropanol were investigated. As shown in the Fig. 1a, OTC exhibited a low fluorescence response in ultrapure water and Tris

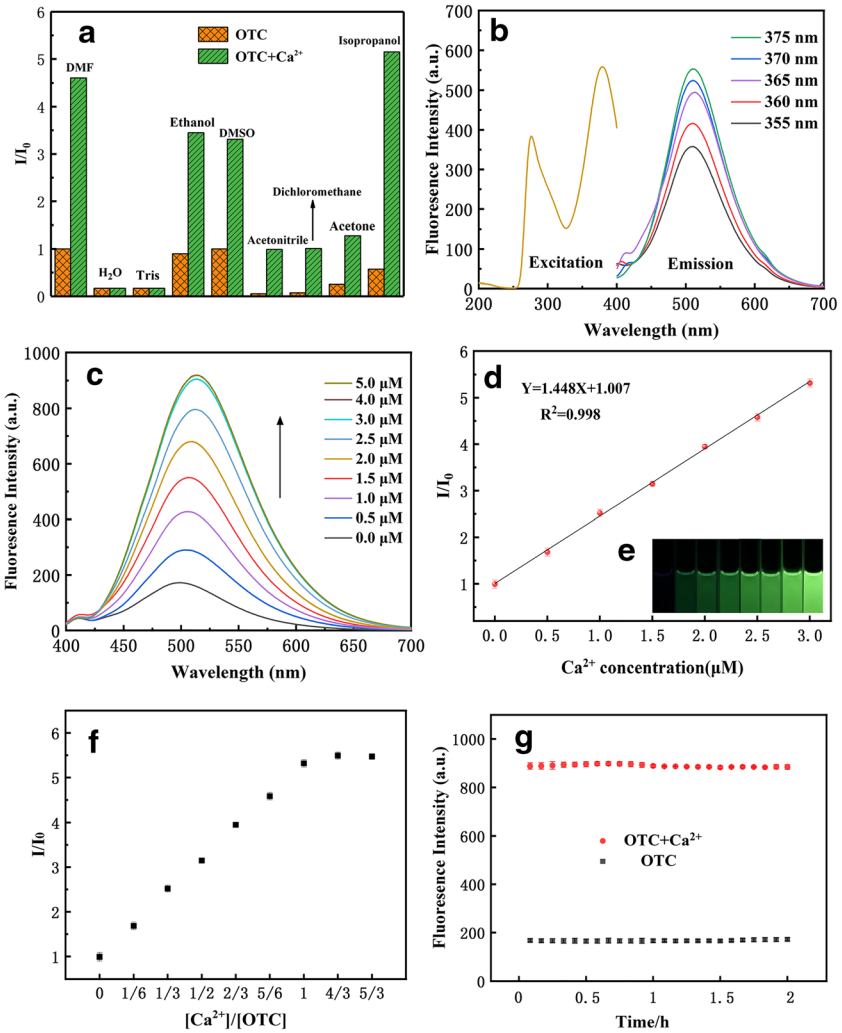

Fig. 1 **a** From left to right: DMF, aqueous solution, Tris buffer (10 mM), ethanol, DMSO, acetonitrile, dichloromethane, acetone and isopropanol. I_0 and I are the fluorescence intensity of OTC at 500 nm and OTC + Ca^{2+} at 510 nm (λ_{ex} = 365 nm), respectively. **b** Excitation and emission spectra (the positions of the excitation wavelength are 355 nm, 360 nm, 365 nm, 370 nm, 375 nm respectively) of the mixture of OTC and Ca^{2+} in DMF. **c** Fluorescence spectra of the probe OTC (3 μM) in the presence of different concentrations of Ca^{2+} in DMF. **d** The linear relationship between the fluorescent intensity of OTC probe and Ca^{2+} concentration. I and I_0 are the fluorescence intensity of OTC at 500 nm and OTC + Ca^{2+} at 510 nm (λ_{ex} = 365 nm), respectively. **e** The visualization photograph for OTC and addition of different concentrations about Ca^{2+} was taken under illumination by a 365 nm UV portable lamp in the dark. **f** Fluorescence intensity ratio of the probe OTC (3 μM) before and after the addition of Ca^{2+} (0–5 μM). **g** The fluorescence intensity of OTC at 3 μM with and without of Ca^{2+} with time. The detection time is limited to 2 h

buffer solution (pH = 7), in which there was no fluorescence-enhanced response with the addition of Ca^{2+}. However, the fluorescence of OTC can be enhanced significantly when it dissolved in organic solvent DMF or ethanol, which can be attributed to its instability in ultrapure water and Tris buffer solution. It also exhibited good response to calcium ions in other organic solvents including DMSO and isopropanol. In the solution system of acetonitrile, methylene chloride, and acetone, no significant fluorescence enhancement was observed. The final concentration of OTC and calcium ions was 3 μM, and the conditions remained consistent. It is possible that the hydroxyl group forms hydrogen bonds with water in aqueous solution which damaged the sensitive response of OTC to Ca^{2+}, while for the organic solvent DMF, it maintained the unhydrolyzed structure of OTC. By evaluating the experimental conditions, the solvent with high polarity and density was found to enable the complex molecules to maintain stable fluorescence performance, and thus the best experimental conditions were obtained.

Fluorescence Determination of Ca^{2+}

OTC dissolved in DMF displays absorption and emission maxima at 380 and 510 nm, respectively, with a relatively large Stokes shift (130 nm). Furthermore, as the excitation wavelength varied from 355 nm to 375 nm, the emission peak of the mixture at 510 nm in the DMF solution did not change, indicating that it is not an

excitation wavelength dependent emission spectroscopy system (Fig. 1b). The excitation of the adjacent wavelength at 365 nm can only change the intensity of the fluorescence, and does not affect the experimental results which previously proposed.

The fluorescence response time of the probe OTC to Ca^{2+} was studied before the sensitivity study to specifically determine the sensing performance of OTC. With the addition of Ca^{2+}, the fluorescence was immediately enhanced and remained unchanged even with increased incubation time was further increased, indicating that the equilibrium between OTC and Ca^{2+} was rapid and stable (Fig. 1c). Clearly, the fluorescence intensity ratio of I/I_0 illustrates a superior linear correlation ($R = 0.998$) with Ca^{2+} concentration in the range of 0–3 μM (Fig. 1d), which was estimated according to the definition of the three times of the blank signal deviation (3σ). And the limit of detection (LOD) was obtained at 125 nM. In addition, this fluorescence enhancement could be easily visualized with the probe solution changing in fluorescence color from darkness to intense green under a 365 nm UV lamp (Fig. 1e), which indicates a significant change in chromatic aberration. In the same period, fluorescence data was used to explore the ratio of 1:1 as support data (Fig. 1f). Also, it was also evidenced by recording the fluorescence of OTC and OTC+ Ca^{2+} for 2 h as shown in Fig. 1g. The UV–vis absorption spectra of OTC (30 μM) with Ca^{2+} (0–50 μM) in DMF (Fig. 2a) that showed a proportional coordination pattern. Clearly, the reaction of OTC with Ca^{2+} results in a new absorption band at 384 nm accompanied by gradually decreasing of the original absorption peak at 369 nm, leading to the formation of an isosbestic point at 366 nm, indicating the formation of a new Ca complex. Here, the chart clearly shows the saturation at 30 μM, indicating a 1:1 coordination of compound OTC with Ca^{2+} (Fig. 2b).

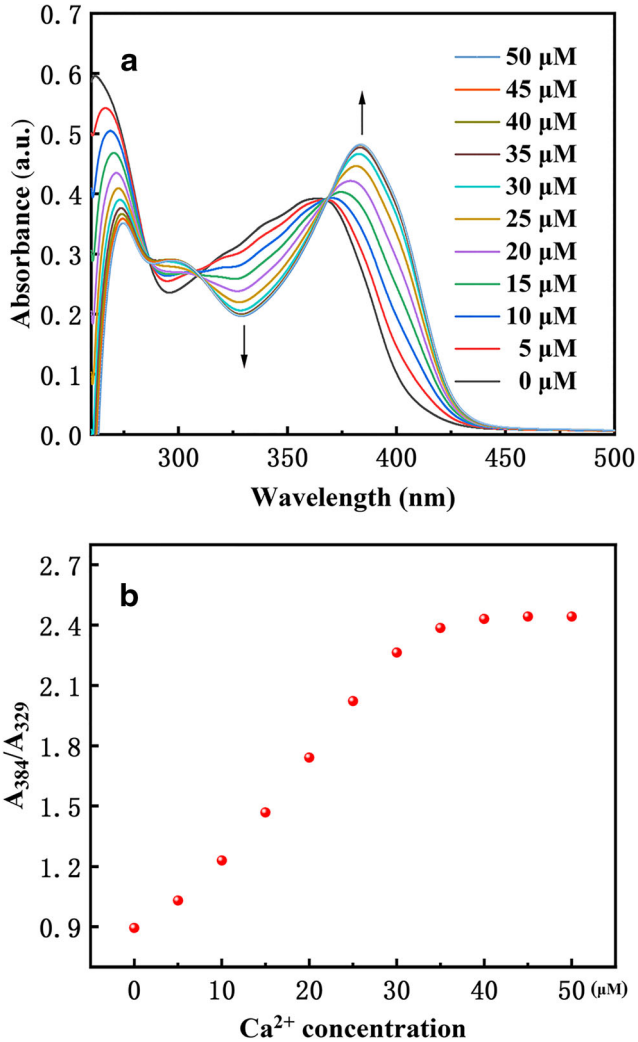

Fig. 2 **a** UV–vis absorption spectra of OTC (30 μM) with Ca^{2+} (0–50 μM) in DMF. **b** Response of the signal to Ca^{2+} under increasing concentrations (0–50 μM) with a concentration of OTC at 30 μM

Fluorescence Quantum Yield Measurement

Fluorescence quantum yield of OTC was calculated using the following equation. Where ΦF stands for fluorescence quantum yields, Abs and ΣF represent the absorbance at the excitation wavelength and the measured integrated fluorescence intensity, and η is the refractive index of the solvent used [29–31]. It is known that the refractive index of ethanol is 1.36242, while the refractive index of DMF is 1.3331. Rhodamine 6G ($\Phi_F = 95\%$) in ethanol was selected as standards.

$$\varphi F_{sample} = \varphi F_{standard} \cdot \frac{Abs_{standard}}{Abs_{sample}} \cdot \frac{\sum F_{sample}}{\sum F_{standard}} \cdot \frac{\eta^2_{sample}}{\eta^2_{standard}}$$

At the same time, it can be proved that the increase of OTC concentration will slightly increase the fluorescence. The fluorescence quantum yields of OTC in DMF was measured to be 7.34% using Rhodamine 6G as a reference.

Binding Constant

The binding constant K of the complex was calculated with a linear relationship by the Benesi-Hildebrand method. Where

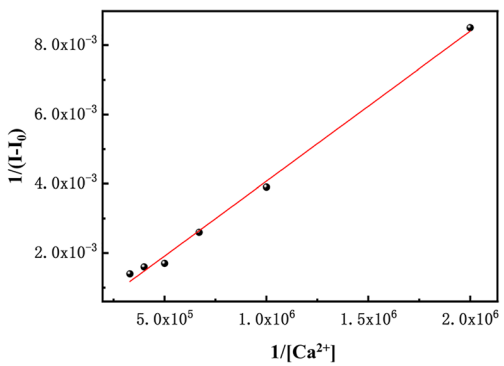

Fig. 3 Benesi-Hildebrand plot based on a 1:1 association stoichiometry between the OTC with Ca^{2+}

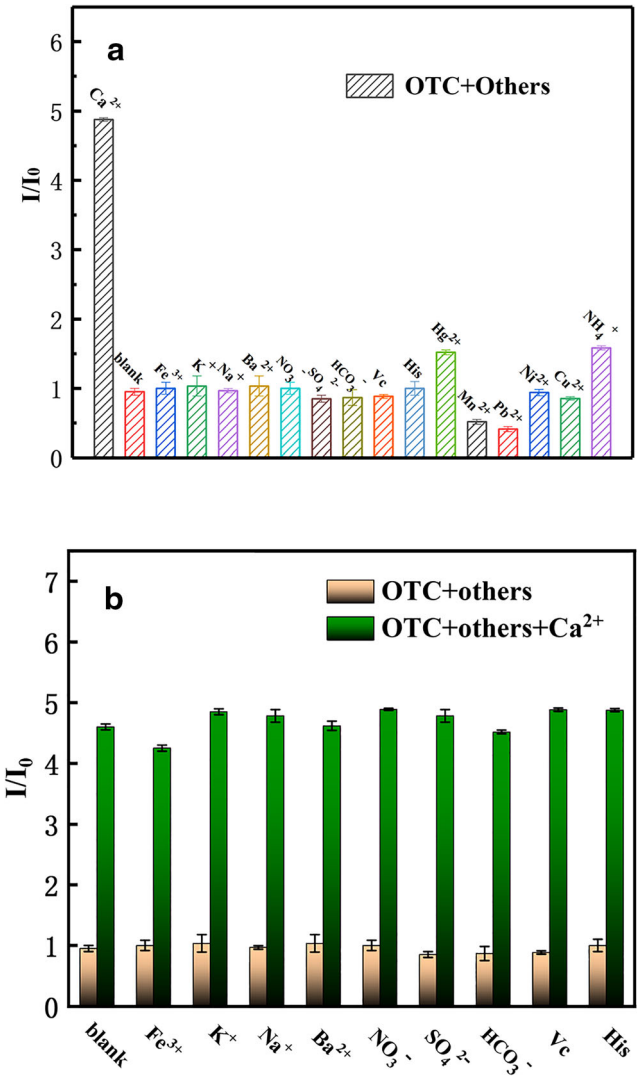

Fig. 4 **a** Fluorescence responses of OTC (3 μM) to various species in DMF including Fe^{3+}, K^+, Na^+, Ba^{2+}, carbonate ion (NO_3^-), sulfate ion (SO_4^{2-}), bicarbonate ion (HCO_3^-), L-ascorbic acid (Vc) and L-histidine (His), Hg^{2+}, Mn^{2+}, Pb^{2+}, Ni^{2+}, Cu^{2+} and NH_4^+. The concentration of added substances was 3 μM. **b** Anti-interference exploration of the probe OTC (3 μM) to coexisting Fe^{3+}, K^+, Na^+, Ba^{2+}, carbonate ion (NO_3^-), sulfate ion (SO_4^{2-}), bicarbonate ion (HCO_3^-), L-ascorbic acid (Vc), and L-histidine (His) in DMF. The concentration of interfering substances was 3 μM

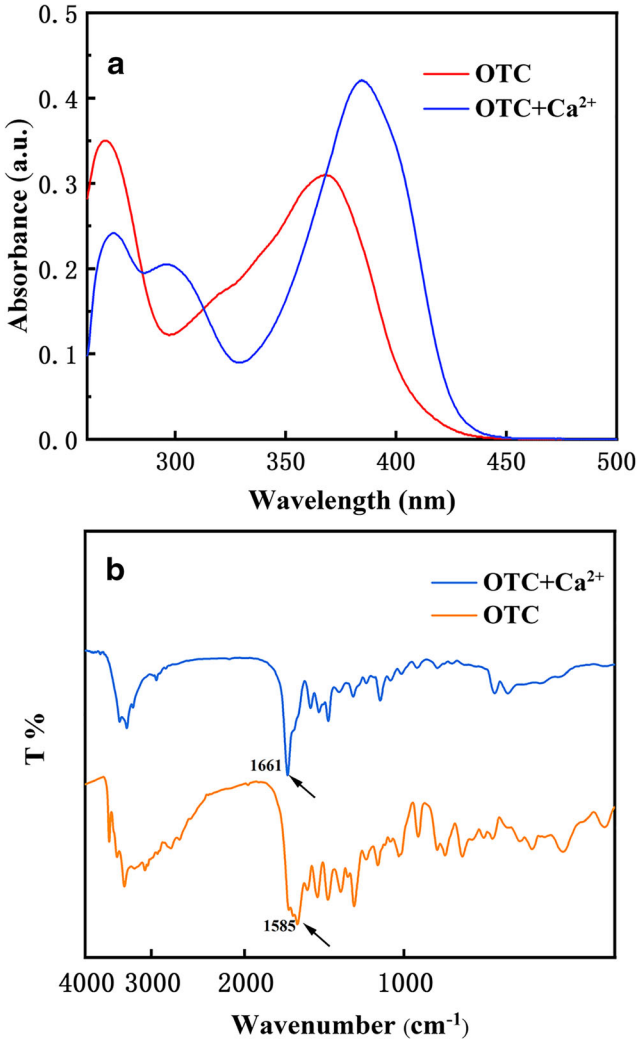

Fig. 5 **a** UV–vis absorption spectra of compound OTC without and with the addition of Ca^{2+}. **b** FTIR spectrum of compound OTC and the mixture of OTC + Ca^{2+} against the background of potassium bromide

F_{min} is the fluorescence intensity of OTC, F_{max} is the intensity measured with an excess of Ca^{2+}, F is the intensity within a linear relationship, and K is the binding constant. The value of K was obtained from a plot of $1/(F_{max} - F)$ against $1/[Ca^{2+}]$ where K is equal to the intercept / slope [32–34].

$$\frac{1}{F-F_{min}} = \frac{1}{K(F_{max}-F_{min})[Ca^{2+}]} + \frac{1}{F_{max}-F_{min}}$$

Here, again, the binding constant of OTC to Ca^{2+} ions was obtained by the actual results of fluorescence titration and the related Benesi-Hildebrand method equation. The K value is calculated from the slope by plotting and fitting the obtained data. More importantly, within this range, it was found that $1/I\text{-}I_0$ is liner to $1/[Ca^{2+}]$ ($R^2 = 0.994$), indicating that OTC is very useful in determining the concentration of Ca^{2+}. The binding constant (K) derived from the fluorescence titration data of OTC to Ca^{2+} in the DMF solution was calculated to be $5.77 \times 10^4\ M^{-1}$ (Fig. 3), which suggested that OTC exhibited good binding capacity with Ca^{2+}.

Effects of the Probe Concentration on the Sensitivity

Fluorescence responses of OTC (3 μM) to various ions in DMF including Fe^{3+}, K^+, Na^+, Ba^{2+}, carbonate ion (NO_3^-), sulfate ion (SO_4^{2-}), bicarbonate ion (HCO_3^-), L-ascorbic acid (Vc), L-histidine (His), Hg^{2+}, Mn^{2+}, Pb^{2+}, Ni^{2+}, Cu^{2+} and NH_4^+ were investigated to confirm the unique fluorescence response of Ca^{2+} and OTC as shown in Fig. 4a. The concentration of the added

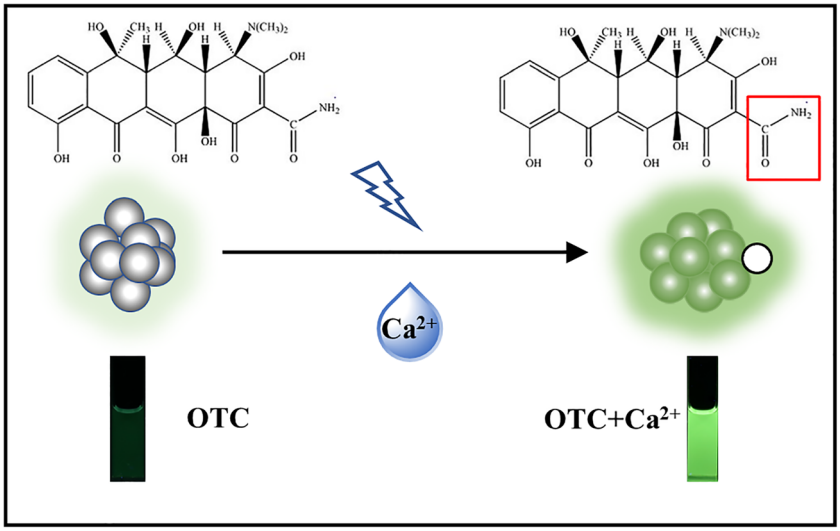

Scheme 1 Sensing process based on the complexation under the excitation wavelength of 365 nm

substances was 3 μM. Only the addition of Ca^{2+} resulted in a significant fluorescence enhancement, and no remarkable changes in the fluorescence of OTC were observed upon the addition of other substances [35, 36]. To investigate the potential interference of these coexisting substances, furthermore, we measured the fluorescence response of OTC toward Ca^{2+} in the presence of mixed coexisting substances with the concentration at 3 μM. As shown in Fig. 4b, all of the coexisting substances have little effects on the detection of Ca^{2+}. These results suggested that the compound OTC is highly selective to Ca^{2+} over other relevant species.

Mechanism Study

Detailed characterization was performed to determine its reaction performance by UV-Vis spectra and Fourier transform infrared (FTIR) spectroscopy. Figure 5a showed the UV − Vis absorption spectra of OTC in the absence and presence of Ca^{2+}. Clearly, the reaction of OTC with Ca^{2+} results in a new absorption band at 384 nm accompanied by gradually decrease of the original absorption peak at 369 nm, indicating the formation of the new Ca complex. The FTIR spectra of the compound OTC, calcium chloride and reacted mixtures were shown in Fig. 5b. The peak at about 3400 cm^{-1} was observed due to the stretching of the O-H groups of OTC. The C=O group stretching vibration of amid corresponded to the peak at approximately 1585 cm^{-1}. Nevertheless, the shift of distinctive peak, such as C=O groups, suggested there was a bonding reaction here in the process [37].

Before as we know, tetracycline derivatives have similar structure, but its chemical properties are different. Different position of hydroxyl group of tetracycline may affect its coordination performance which making it a good ligand exhibiting rich coordination site, such as dimethylamino and phenol-diketone group [38]. The protonation state of the compound explains the inconsistency between the binding sites of tetracycline and metal ions. In a certain solution environment, the proton dissociates from the tetracycline compound, and metal ions would choose an optimum binding site to form a stable complex [39]. It was observed that the hydration of metal ions affected the state of OTC, and it was aggregated in the presence of Ca^{2+}. In addition, the solubility of metal complex is greater than that of the OTC, suggesting that Ca^{2+} somehow increases the solubility of OTC in solution [40]. OTC is known for its different ionized states in different solution conditions, and its ion binding patterns are diverse. As mentioned above, the fluorescence and absorption data showed that Ca^{2+} binds with OTC at a 1:1 stoichiometric rate, suggesting that the probe solution depends on the ionic binding pattern. The results showed that OTC coordinated with Ca^{2+} to form a stable complex in DMF, which exhibited

Table 1 Test of Ca^{2+} spiked in actual samples

Samples	Spiked (μM)	Detected (μM)	Recovery (%)	RSD (%, $n = 3$)
Tap water	1	1.04	104%	2.3
	3	3.10	103%	1.4
River water	1	1.19	119%	3.3
	3	3.23	107%	3.7
Mineral water	1	1.05	105%	6.4
	3	3.13	104%	2.4

significant fluorescence enhancement accordingly [41]. Sensing process based on the complexation under the excitation wavelength of 365 nm was showed in Scheme 1.

Test of Ca^{2+} in Real Water Sample

To assess the potential application of the probe OTC for Ca^{2+} detection in real water systems, the recovery experiment was carried out in three kinds of water samples including tap water, river water and mineral water which were obtained from local place. The actual detection is carried out in with different contents of Ca^{2+}. After pre-treatment of sedimentation and suspension, the water sample spiked with different amounts of Ca^{2+} was added the same concentration of OTC, and the fluorescence of the solution was then recorded. The relative standard deviations (RSD) were obtained by repeating the experiment two times under the same conditions. As shown in Table 1, the recoveries of various known concentrations of added Ca^{2+} were obtained from 103% to 109% in actual samples. Briefly, the relative standard deviations (RSD) were in the range of 1.4% to 6.7% which was generally satisfactory, showing the reliability of the probe OTC for Ca^{2+} determination in real samples.

Conclusion

In summary, we showed that oxytetracycline can be used as a highly sensitive fluorescent probe for detecting Ca^{2+} by the coordination effect to form a stable complex. A good limit of detection at 125 nM was obtained, which was favourable for sensitive and selective detection of Ca^{2+}. The method was further applied to the living water system, which was analysed to evaluate the accuracy and applied of the present method. The strategy with unique fluorescence enhancement reported here definitely facilitates the evolution of portable and real-time calcium monitoring for visual identification application.

Acknowledgments This work was supported by the National Natural Science Foundation of China (2177504, 21675158, 21602151), National Key Research and Development Program of China (2017YFA0207003).

Compliance with Ethical Standards

Conflict of Interest The authors declare that they have no conflict of interest.

References

1. Matthews KA, Grottoli AG, McDonough WF, Palardy JE (2008) Upwelling, species, and depth effects on coral skeletal cadmium-to-calcium ratios (Cd/Ca). Geochim Cosmochim Acta 72(18):4537–4550. https://doi.org/10.1016/j.gca.2008.05.064
2. Gao M, Li Y, Chen X, Li S, Ren L, Tang BZ (2018) Aggregation-induced emission probe for light-up and in situ detection of calcium ions at high concentration. ACS Appl Mater Interfaces 10(17):14410–14417. https://doi.org/10.1021/acsami.8b00952
3. Lin Y, Zheng Y, Guo Y, Yang Y, Li H, Fang Y et al (2018) Peptide-functionalized carbon dots for sensitive and selective Ca2+ detection. Sensors Actuators B-Chem 273:1654–1659. https://doi.org/10.1016/j.snb.2018.07.073
4. Nemutlu E, Ozaltin N (2005) Determination of magnesium, calcium, sodium, and potassium in blood plasma samples by capillary zone electrophoresis. Anal Bioanal Chem 383(5):833–838. https://doi.org/10.1007/s00216-005-0063-0
5. Zhu Y, Itoh A, Fujimori E, Umemura T, Haraguchi H (2005) Multielement determination of trace metals in seawater by inductively coupled plasma mass spectrometry after tandem preconcentration using a chelating resin. Bull Chem Soc Jpn 78(4):659–667. https://doi.org/10.1246/bcsj.78.659
6. Rodriguez-Gonzalez P, Marchante-Gayon JM, Alonso JIG, Sanz-Medel A (2005) Isotope dilution analysis for elemental speciation: a tutorial review. Spectrochim Acta B 60(2):151–207. https://doi.org/10.1016/j.sab.2005.01.005
7. Calvo D, Bartroli J, del Valle M (2007) Multicomponent titration of calcium plus magnesium mixtures employing a potentiometric electronic-tongue. Anal Lett 40(8):1579–1595. https://doi.org/10.1080/00032710701380780
8. Karita S, Kaneta T (2016) Chelate titrations of Ca2+ and Mg2+ using microfluidic paper-based analytical devices. Anal Chim Acta 924:60–67. https://doi.org/10.1016/j.aca.2016.04.019
9. Liu S, Ding J, Qin W (2018) Current pulse based ion-selective electrodes for chronopotentiometric determination of calcium in seawater. Anal Chim Acta 1031:67–74. https://doi.org/10.1016/j.aca.2018.06.018
10. Stojanovic DD, Milinovic JS, Nikolic-Mandic SD (2007) Interferences from titanium and zirconium during calcium determination by flame spectrometry. J Serbian Chem Soc 72(8–9):821–831. https://doi.org/10.2298/jsc0709821s
11. Stoodley R, Nunez JRR, Bartz T (2014) Field and in-lab determination of Ca2+ in seawater. J Chem Educ 91(11):1954–1957. https://doi.org/10.1021/ed4005722
12. Zhai J, Xie X, Bakker E (2014) Ionophore-based ion-exchange emulsions as novel class of complexometric titration reagents. Chem Commun 50(84):12659–12661. https://doi.org/10.1039/c4cc05754f
13. Venezia M, Alonzo G, Palmisano L (2008) EDTA excess Zn(II) back-titration in the presence of 4-(2-pyridylazo)-resorcinol indicator and naphthol green beta as inert dye for determining Cr(III) as Cr(III)/EDTA complex: application of the method to a leather industry wastewater. J Hazard Mater 151(2–3):356–363. https://doi.org/10.1016/j.jhazmat.2007.05.081
14. Zhai J, Zhu C, Peng X, Xie X (2018) Ionophore-based heterogeneous calcium optical titration. Electroanalysis. 30(4):705–709. https://doi.org/10.1002/elan.201700690
15. Granholm K, Sokalski T, Lewenstam A, Ivaska A (2016) Determination of the stability constant of the calcium binding ligand in black liquor (BL) by potentiometric titration. Holzforschung. 70(8):733–738. https://doi.org/10.1515/hf-2015-0194
16. Pereira CM, Neiverth CA, Maeda S, Guiotoku M, Franciscon L (2011) Complexometric titration with potenciometric indicator to determination of calcium and magnesium in soil extracts. Rev Bras Cienc Solo 35(4):1331–1336. https://doi.org/10.1590/s0100-06832011000400027
17. Rafols C, Bosch E, Barbas R, Prohens R (2016) The Ca2+−EDTA chelation as standard reaction to validate isothermal titration calorimeter measurements (ITC). Talanta. 154:354–359. https://doi.org/10.1016/j.talanta.2016.03.075

18. Rodrigues S, Antunes SC, Correia AT, Nunes B (2018) Oxytetracycline effects in specific biochemical pathways of detoxification, neurotransmission and energy production in Oncorhynchus mykiss. Ecotoxicol Environ Saf 164:100–108. https://doi.org/10.1016/j.ecoenv.2018.07.124
19. Chang PH, Li Z, Jean JS, Jiang WT, Wu Q, Kuo CY, Kraus J (2014) Desorption of tetracycline from montmorillonite by aluminum, calcium, and sodium: an indication of intercalation stability. Int J Environ Sci Technol 11(3):633–644. https://doi.org/10.1007/s13762-013-0215-2
20. Kim C-H, Lee L-P, Min J-R, Lim M-W, Jeong S-H (2014) An indirect competitive assay-based aptasensor for detection of oxytetracycline in milk. Biosens Bioelectron 51:426–430. https://doi.org/10.1016/j.bios.2013.08.003
21. Harja M, Ciobanu G (2018) Studies on adsorption of oxytetracycline from aqueous solutions onto hydroxyapatite. Sci Total Environ 628–629:36–43. https://doi.org/10.1016/j.scitotenv.2018.02.027
22. Zhang H, Fang C, Wu S, Duan N, Wang Z (2015) Upconversion luminescence resonance energy transfer-based aptasensor for the sensitive detection of oxytetracycline. Anal Biochem 489:44–49. https://doi.org/10.1016/j.ab.2015.08.011
23. Wu H, Chen W, Yang H, Wang S, Lim ST, Yao W et al (2016) Improved synthesis dimethylhomoecoerdianthrone (HOCD) and its functionalization through facile amination reactions. Dyes Pigments 130:154–161. https://doi.org/10.1016/j.dyepig.2016.03.016
24. Hosseini M, Mehrabi F, Ganjali MR, Norouzi P (2016) A fluorescent aptasensor for sensitive analysis oxytetracycline based on silver nanoclusters. Luminescence. 31(7):1339–1343. https://doi.org/10.1002/bio.3112
25. Chen H, Peng Y-P, Chen K-F, Lai C-H, Lin Y-C (2016) Rapid synthesis of Ti-MCM-41 by microwave-assisted hydrothermal method towards photocatalytic degradation of oxytetracycline. J Environ Sci-China 44:76–87. https://doi.org/10.1016/j.jes.2015.08.027
26. Tong F, Zhao Y, Gu X, Gu C, Lee CCC (2015) Joint toxicity of tetracycline with copper(II) and cadmium(II) to Vibrio fischeri: effect of complexation reaction. Ecotoxicology. 24(2):346–355. https://doi.org/10.1007/s10646-014-1383-7
27. Li M-J, Zeng T (2019) The deleterious effects of N,N-dimethylformamide on liver: a mini-review. Chem Biol Interact 298:129–136. https://doi.org/10.1016/j.cbi.2018.12.011
28. Loring HS, Luthy NG (1951) The isolation in crystalline form and characterization of the two isomeric cytidylic acids derived from yeast nucleic Acid1. J Am Chem Soc 73(9):4215–4218
29. Yue J, Zhang K, Yu H, Yu L, Hou T, Chen X, Ge H, Hayat T, Alsaedi A, Wang S (2019) Mechanism insights into tunable photoluminescence of carbon dots by hydroxyl radicals. J Mater Sci 54(8):6140–6150. https://doi.org/10.1007/s10853-018-03254-1
30. Yu L, Li Y, Yu H, Zhang K, Wang X, Chen X et al (2018) A fluorescence probe for highly selective and sensitive detection of gaseous ozone based on excited-state intramolecular proton transfer mechanism. Sensors Actuators B-Chem 266:717–723. https://doi.org/10.1016/j.snb.2018.03.175
31. Sun M, Yang X, Zhang Y, Wang S, Wong MW, Ni R, Huang D (2019) Rapid and visual detection and quantitation of ethylene released from ripening fruits: the new use of Grubbs catalyst. J Agric Food Chem 67(1):507–513. https://doi.org/10.1021/acs.jafc.8b05874
32. Hildebrand JH, Benesi HA (1949) Interaction of iodine with aromatic hydrocarbons. Nature. 164(4179):963
33. Wang M-Q, Li K, Hou I-T, Wu M-Y, Huang Z, Yu X-Q (2012) BINOL-based fluorescent sensor for recognition of Cu(II) and sulfide anion in water. J Org Chem 77(18):8350–8354. https://doi.org/10.1021/jo301196m
34. Fu Y, Fan C, Liu G, Pu S (2017) A colorimetric and fluorescent sensor for Cu2+ and F- based on a diarylethene with a 1,8-naphthalimide Schiff base unit. Sensors Actuators B-Chem 239:295–303. https://doi.org/10.1016/j.snb.2016.08.020
35. Liu L, Yu L, Chen X, Yue J, Asiri AM, Marwani HM et al (2017) Synthesis and characterization of binaphthalene-2,2 '-diamine-functionalized gold nanoparticles. J Nanoparticle Resh 19(10). https://doi.org/10.1007/s11051-017-4040-2
36. Yu H, Sun M, Zhang K, Zhu H, Liu Z, Zhang Y et al (2015) A reversible near-infrared pH probes for optical measurements of pH in complete water system and living cells. Sensors Actuators B-Chem 219:294–300. https://doi.org/10.1016/j.snb.2015.05.029
37. Fu B, Ge C, Yue L, Luo J, Feng D, Deng H et al (2016) Characterization of biochar derived from pineapple peel waste and its application for sorption of oxytetracycline from aqueous solution. Bioresources 11(4):9017–9035. https://doi.org/10.15376/biores.11.4.9017-9035
38. Yang X, Zhang S, Yu W, Liu Z, Lei L, Li N et al (2014) Ionic liquid-anionic surfactant based aqueous two-phase extraction for determination of antibiotics in honey by high-performance liquid chromatography. Talanta. 124:1–6. https://doi.org/10.1016/j.talanta.2014.02.039
39. Stephens C, Murai K, Brunings K, Woodward R (1956) Acidity constants of the tetracycline antibiotics. J Am Chem Soc 78(16):4155–4158
40. Eugenia Parolo M, Avena MJ, Pettinari GR, Baschini MT (2012) Influence of Ca2+ on tetracycline adsorption on montmorillonite. J Colloid Interface Sci 368:420–426. https://doi.org/10.1016/j.jcis.2011.10.079
41. Jin L, Amaya-Mazo X, Apel ME, Sankisa SS, Johnson E, Zbyszynska MA, Han A (2007) Ca2+ and Mg2+ bind tetracycline with distinct stoichiometries and linked deprotonation. Biophys Chem 128(2–3):185–196. https://doi.org/10.1016/j.bpc.2007.04.005